



澳門科技大学  
MACAU UNIVERSITY OF SCIENCE AND TECHNOLOGY

# Kelvin-Helmholtz Instability and Its Applications on the Space Environment of Earth and Mars

– Group Meeting of the Planetary Space Physics

**WANG,XING**

State Key Laboratory of Lunar and Planetary Sciences, Space Science Institute,  
Macau University of Science and Technology



Oct.16, 2020. Macau, China



# Outline

## Introduction of Kelvin-Helmholtz Instability

Basic Concept of Kelvin-Helmholtz Instability

Natural Phenomena of Kelvin-Helmholtz Instability

Magnetohydrodynamics(MHD) Kelvin-Helmholtz Instability

## Applications on the Space Environment of Earth and Mars

Earth

Mars

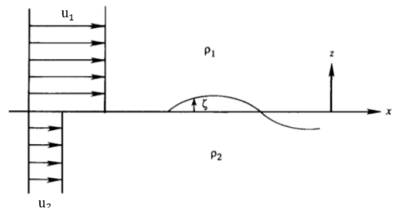
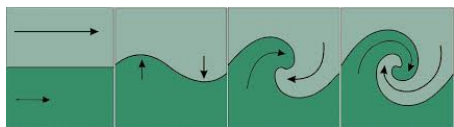
## Further Works About Study of KHI on the Martian Space Environment



# Basic Concept of Kelvin-Helmholtz Instability

- Kelvin-Helmholtz instability (KHI) was first studied by Hermann von Helmholtz in 1868 and by William Thomson (Lord Kelvin) in 1871;
- incompressible and inviscid fluids;
- relative and irrotational motion;
- the velocity  $u$  and density  $\rho$  profiles are uniform in each fluid layer;
- $u$  and  $\rho$  are discontinuous at the interface: shear flow;
- The condition of instability:

$$(u_1 - u_2)^2 > \frac{g(\rho_2^2 - \rho_1^2)}{k\rho_1\rho_2}$$





# Natural Phenomena of KHI: Arts



Hiroshige Utagawa "Vortices in the Konaruto stream"



Vincent Van Gogh "La Nuit Etoilee"



# Natural Phenomena of KHI: Ocean and Cloud

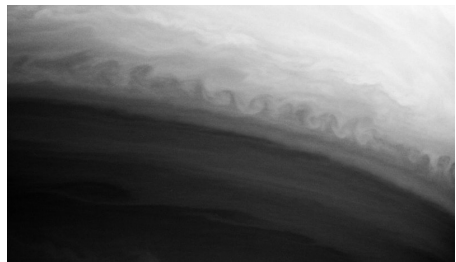




# Natural Phenomena of KHI: Giant Planets



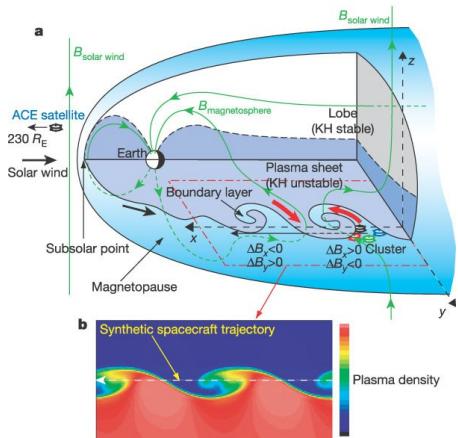
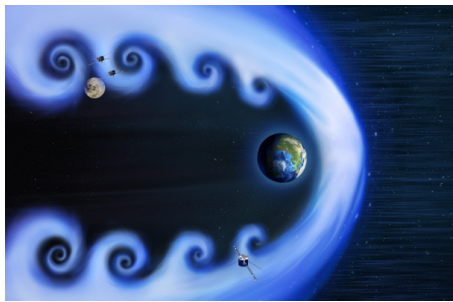
Jupiter, great spot, Voyager 2(NASA)



Saturn pictured by Cassini(NASA)



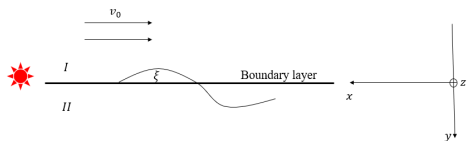
# Natural Phenomena of KHI: Space Plasma



Hasegawa et al. 2004

# Mathematical Model of MHD KHI

- Considering a hydromagnetic perturbation near a boundary of discontinuous flow velocity;
- Assuming incompressible ideal MHD perturbations;



- Linearized MHD equations:

$$\nabla \cdot \mathbf{v} = 0$$

$$m_i n \frac{d\mathbf{v}}{dt} = \mathbf{J} \times \mathbf{B} - \nabla p$$

$$\mathbf{E} + \mathbf{v} \times \mathbf{B} = \eta \mathbf{J}$$

$$\nabla \times \mathbf{B} = \mu_0 \mathbf{J}$$

$$\frac{\partial \xi}{\partial t} = \mathbf{v}_1$$

$$m_i n_0 \ddot{\xi} = \frac{1}{\mu_0} [(\nabla \times \mathbf{B}_1) \times \mathbf{B}_0 + (\nabla \times \mathbf{B}_0) \times \mathbf{B}_1] - \nabla p_1$$

$$\mathbf{B}_1 = \nabla \times (\xi \times \mathbf{B}_0) = (\mathbf{B}_0 \cdot \nabla) \xi - (\xi \cdot \nabla) \mathbf{B}_0 - \mathbf{B}_0 (\nabla \cdot \xi)$$



■ Considering  $\nabla \cdot \mathbf{B}_1 = \nabla \cdot \mathbf{B}_0 = 0$  and  $\nabla \cdot \mathbf{v}_1 = \nabla \cdot \boldsymbol{\xi} = 0$ , we can get:

$$\nabla^2 \tilde{p}_1 = \frac{1}{\mu_0} \nabla \cdot [(\mathbf{B}_0 \cdot \nabla) \mathbf{B}_1 + (\mathbf{B}_1 \cdot \nabla) \mathbf{B}_0] - \nabla \cdot (m_i n_0 \ddot{\boldsymbol{\xi}}) = 0$$

where  $\tilde{p}_1$  is the total pressure given by  $\tilde{p}_1 = \frac{\mathbf{B}_1 \cdot \mathbf{B}_0}{\mu_0} + p_1$ ;

■ This is a Laplace equation, the wave-like solution is given by:

$$\tilde{p}_1 = p_0 e^{-\kappa|y|} e^{i(k_x x + k_z z - \omega t)}, \quad \kappa = \sqrt{k_x^2 + k_z^2}$$

■ Substituting the above solution into the linearized MHD equations, we can get:

$$[\mu_0 m_i n_0 \omega^2 - (\mathbf{k} \cdot \mathbf{B}_0)^2] \boldsymbol{\xi} = \mu_0 \nabla \tilde{p}_1 + \mathbf{c}$$

where

$$\mathbf{c} = (\mathbf{B}_0 \cdot \nabla)[(\boldsymbol{\xi} \cdot \nabla) \mathbf{B}_0 + \mathbf{B}_0 (\nabla \cdot \boldsymbol{\xi})] - (\mathbf{B}_1 \cdot \nabla) \mathbf{B}_0$$

vanishes in a uniform plasma. In that case:

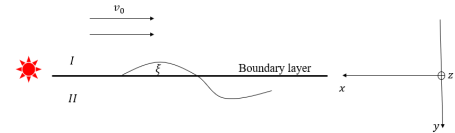
$$\boldsymbol{\xi} = \frac{\nabla \tilde{p}_1}{m_i n_0 [\omega^2 - (\mathbf{k} \cdot \mathbf{v}_A)^2]}$$

where  $\mathbf{v}_A = \frac{\mathbf{B}_0}{\sqrt{\mu_0 m_i n_0}}$  is Alfvén velocity, and  $\mathbf{k} = k_x \mathbf{e}_x + k_z \mathbf{e}_z$ .



- I:  $y < 0$ ; II:  $y > 0$ ;
- $\omega_I$  is Doppler shifted with respect to  $\omega_{II}$ :  $\omega_I = \omega - \mathbf{k} \cdot \mathbf{v}_0$ ,  $\omega_{II} = \omega$ ;
- Total pressure  $\tilde{p}_1$  is continuous at the boundary;
- We can get the dispersion relation:

$$\frac{1}{n_{0I}[(\omega - \mathbf{k} \cdot \mathbf{v}_0)^2 - (\mathbf{k} \cdot \mathbf{v}_A)_I^2]} + \frac{1}{n_{0II}[\omega^2 - (\mathbf{k} \cdot \mathbf{v}_A)_{II}^2]} = 0$$



Or:

$$(n_{0I} + n_{0II})\omega^2 - 2n_{0I}(\mathbf{k} \cdot \mathbf{v}_0)\omega + n_{0I}[(\mathbf{k} \cdot \mathbf{v}_0)^2 - (\mathbf{k} \cdot \mathbf{v}_A)_I^2] - n_{0II}(\mathbf{k} \cdot \mathbf{v}_A)_{II}^2 = 0$$

- The solution for  $\omega$  are:

$$\omega = \frac{1}{n_{0I} + n_{0II}} \left[ n_{0I}(\mathbf{k} \cdot \mathbf{v}_0) \pm \sqrt{\Delta} \right]$$

- $\omega$  will be a complex number  $\omega = \omega_r + i\omega_i$  when:

$$\Delta = \left( \frac{1}{n_{0I}} + \frac{1}{n_{0II}} \right) [n_{0I}(\mathbf{k} \cdot \mathbf{v}_A)_I^2 + n_{0II}(\mathbf{k} \cdot \mathbf{v}_A)_{II}^2] - (\mathbf{k} \cdot \mathbf{v}_0)^2 < 0$$

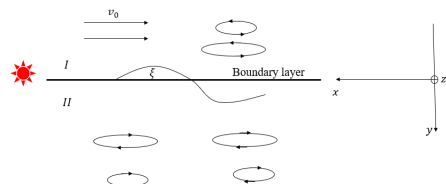
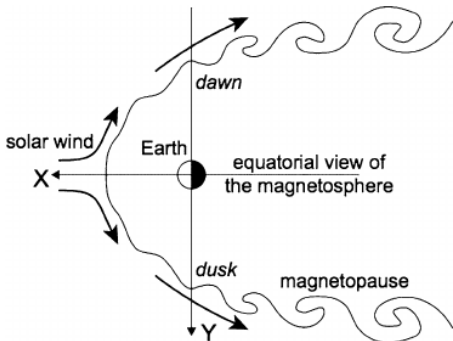


## The condition of KHI:

$$(\mathbf{k} \cdot \mathbf{v}_0)^2 > \left( \frac{1}{n_{0I}} + \frac{1}{n_{0II}} \right) [n_{0I}(\mathbf{k} \cdot \mathbf{v}_A)_I^2 + n_{0II}(\mathbf{k} \cdot \mathbf{v}_A)_{II}^2]$$

KHI occurs more easily when:  $(\mathbf{k} = k_x \mathbf{e}_x + k_z \mathbf{e}_z)$

$$\mathbf{k} \perp \mathbf{B}_0 \quad or \quad \mathbf{k} \parallel \mathbf{v}_0$$





# KHI on the Earth's magnetosphere

## Why study KHI

- **How the solar wind plasma, momentum and energy enter into the Earth's magnetosphere?**
- Several scenarios of plasma transport: magnetic reconnection, diffusive particle transport via turbulence, anomalous transport due the conversion of KH surface waves to kinetic Alfvén waves;
- **Southward IMF:**
  1. Magnetic reconnection occur at the subsolar magnetopause;
  2. Leading to storage of magnetic energy and reconnection in the magnetotail;
- **Northward IMF:**
  1. Magnetic reconnection occur mostly at tailward of the cusps;
  2. Solar wind plasma penetration is observed at the Low Latitude Boundary Layer(LLBL) and in the central plasma sheet;
  3. Other physical phenomena have been proposed: high-latitude reconnection and the KHI.

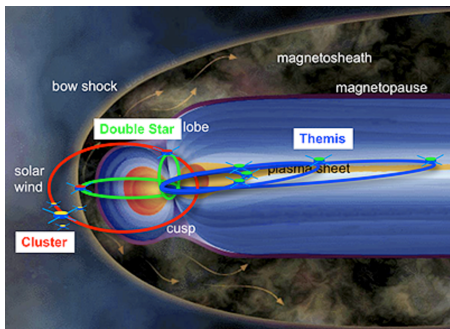


## Questions

- Does KHI lead to the development of rolled-up vortices along the magnetopause?
- Are they rare or a common feature?
- Is there a dawn–dusk asymmetry? if yes what causes it?
- Does the KHI only occurs during Northward IMF and near the LLBL(the Low Latitude Boundary Layer)?
- What are the physical mechanisms within a KHI vortex allowing magnetosheath plasma to enter or magnetospheric plasma to exit the magnetosphere?
- How does this phenomenon develop from birth to collapse along the magnetopause?
- How is magnetic reconnection initiated within KH rolled-up vortices?
- What is the contribution of the KHI vs. magnetic reconnection in terms of plasma entry?

# KHI on the Earth's magnetosphere

## Earth's Magnetospheric Missions:

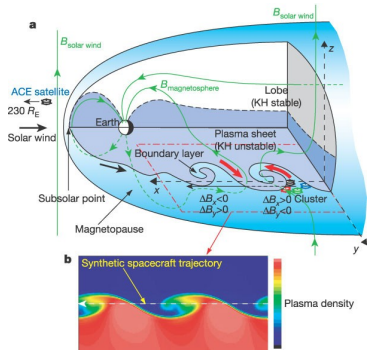


Orbit of Cluster, THEMIS and Double Star

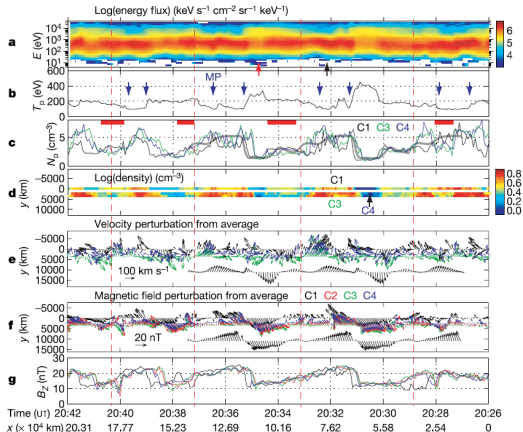


Orbit of Geotail mission

- **THEMIS:** The Time History of Events and Macroscale Interactions during Substorms.



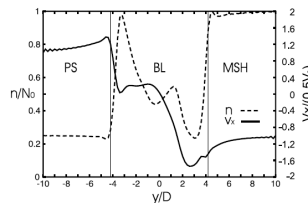
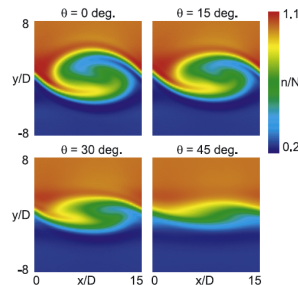
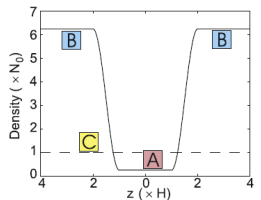
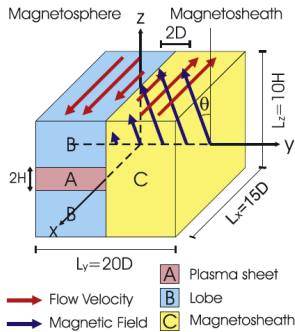
Hasegawa et al. 2004



Hasegawa et al. 2004

- 20 November 2001, northward IMF;
- KH waves can roll-up and evolve into  $4 - 5.5 \times 10^4$  km wide vortices.

## ■ Tenuous plasma must rotate faster than a denser plasma:



Takagi et al. 2006

WANG,XING • Group Meeting-Kelvin-Helmholtz Instability •

Takagi et al. 2006



## These vortices are not rare under northward IMF conditions:

**Table 1.** KHI Events Observed by THB and THC From 2008 to 2009

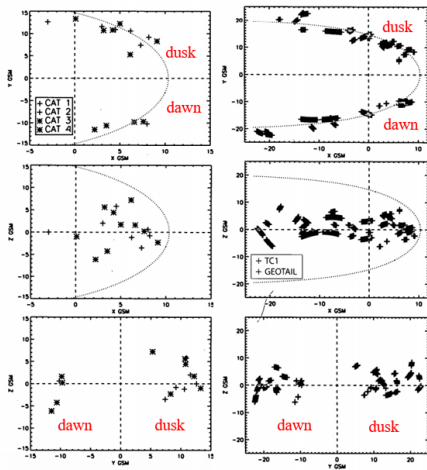
Probe	Date (yyyy-mm-dd)	Time Interval (hhmm-hhmm)	GSM Position ( $R_E$ )	$T_{KH}$ (s)	$V_{ph}$ (km/s)	$\lambda_{KH}$ ( $R_E$ )	IMF (nT)	CA (degree)	$V_{SW}$ (km/s)
THC	2008-4-13	0240-0440	(-5.1, 17.2, 1.6)	325	111	5.7	(-0.1, 3.0, 2.1)	50	577
THC	2008-5-1	1150-1240	(-4.5, 18.5, -2.3)	242	170	6.5	(-3.6, 1.8, 2.1)	39	469
THB	2008-5-15	1430-1510	(-4.2, 16.9, 1.2)	115	174	3.1	(5.5, -2.2, 1.4)	-55	331
THB	2008-9-13	1212-1237	(4.8, -11.6, 0.1)	95	141	2.1	(1.6, 1.0, 2.1)	25	313
THC	2008-9-17	1205-1240	(7.9, -10.4, 1.1)	147	117	2.7	(2.2, -1.0, 4.5)	-12	431
THB	2008-9-17	1310-1400	(5.4, -13.1, 0.1)	119	177	3.3	(2.7, -0.9, 4.6)	-10	430
THC	2008-11-6 <sup>a</sup>	0852-0952	(-0.3, -15.3, 4.6)	134	156	3.3	(2.1, -0.9, 1.5)	-31	288
THC	2008-11-18	0720-0800	(-2.3, -17.0, 3.4)	174	129	3.5	(-1.0, -1.0, 3.1)	-17	348
THB	2009-4-6	0710-0835	(-19.4, 25.0, 3.3)	448	203	14.3	(0.7, 1.8, 2.2)	39	405
THC	2009-5-29	0000-0040	(4.5, 14.9, 1.9)	258	120	4.9	(-1.3, -1.3, 0.6)	-67	404
THC	2009-6-6	0023-0113	(6.5, 12.6, 0.4)	95	152	2.3	(-0.8, -3.2, 2.8)	-48	327
THB	2009-10-3	0740-0820	(0.9, -16.0, 4.5)	204	168	5.4	(-0.6, 0.2, 2.0)	6	325
THB	2009-10-12	0200-0245	(10.6, 5.2, 1.7)	354	77	4.3	(-1.0, -3.1, 2.6)	-47	416
THB	2009-11-2	1850-1950	(-9.8, -19.9, -1.0)	212	248	8.3	(2.8, -3.1, 2.0)	-58	349

**Table 2.** Instruments Providing the Magnetic Field and Plasma Measurements and Counts of the KH Wave Events for Each Spacecraft<sup>a</sup>

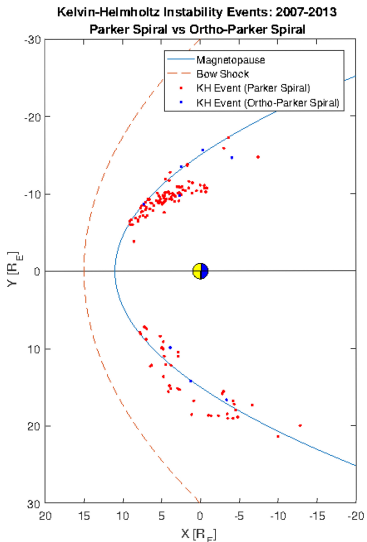
Spacecrafts	Magnetic Field	Plasma	Count
Geotail	Magnetic Field Experiment (MGF) [Kokubun et al., 1994]	Low Energy Particle Experiment (LEP) [Mukai et al., 1994]	20
TC – 1	Flux Gate Magnetometer (FGM) [Carr et al., 2005]	Hot Ion Analyzer (HIA) [Rème et al., 2005]	17
Cluster	Flux Gate Magnetometer (FGM) [Balogh et al., 2001]	Cluster Ion Spectrometry (CIS) [Rème et al., 2001]	5
THEMIS	FluxGate Magnetometer (FGM) [Auster et al., 2008]	ElectroStatic Analyzer (ESA) [McFadden et al., 2008]	14



## Possible dawn-dusk asymmetry:

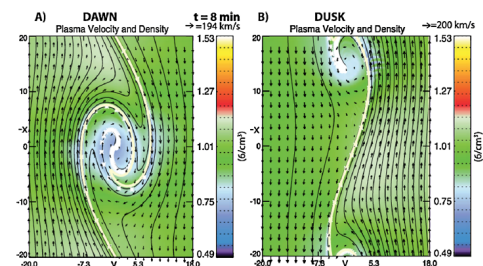
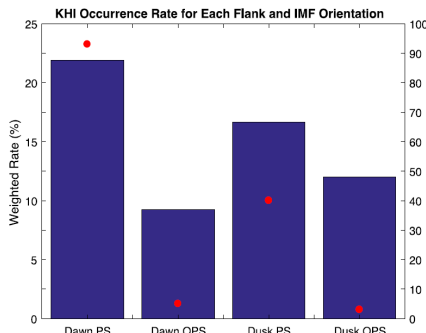


Taylor et al. 2012



Henry et al. 2017

- Asymmetric heating: temperature at the dawnside plasma sheet denser and hotter 30 – 40% than duskside (Hasegawa et al. 2003; Wing et al. 2005);



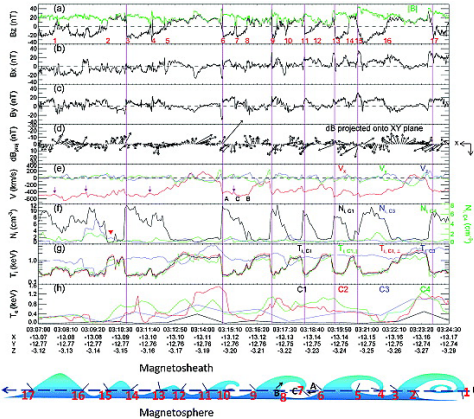
Masson and Nykyri 2018

Masson and Nykyri 2018

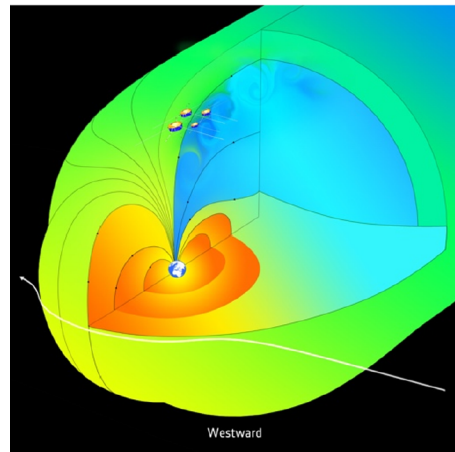
- The dawn-favoured asymmetry of the KH waves and ion scale waves may therefore explain the origin of the observed plasma sheet temperature and density asymmetry.



## ■ Southward IMF and downward IMF conditions:

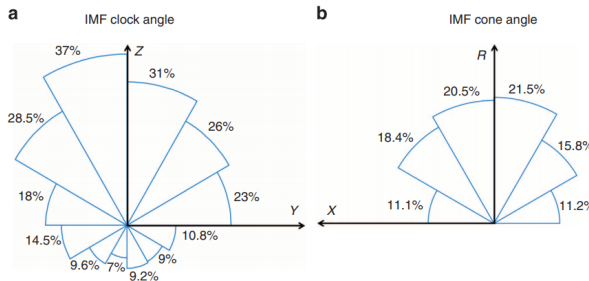


Hwang et al. 2011



Masson and Nykyri 2018

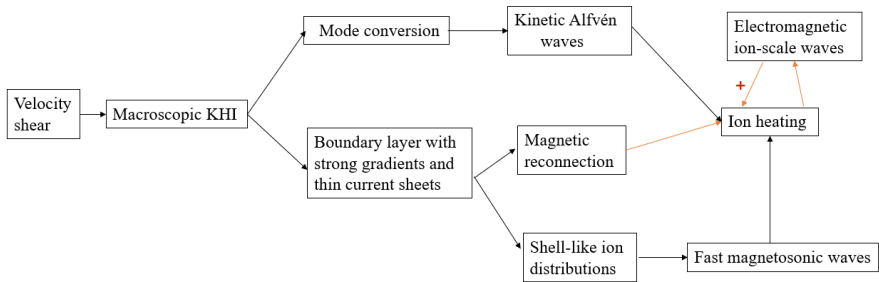
- When velocity shear and magnetic shear are not aligned, the KH modes and tearing modes are unstable;
- the KHI onset condition can be satisfied more often for northward than for southward IMF conditions.



Kavosi and Raeder 2015

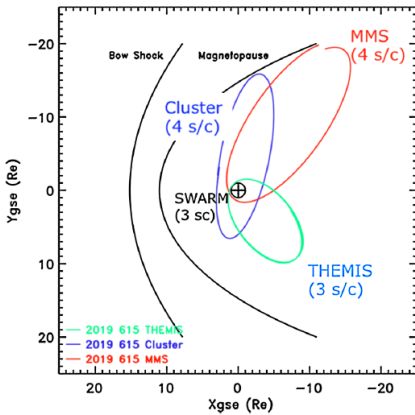
- clock angle =  $\arctan \frac{B_y}{B_z}$ , cone angle =  $\arccos \frac{B_x}{B}$ ,  $R = \sqrt{Y^2 + Z^2}$ ;
- Samples: 7 years, THEMIS crossed magnetopause during 960h, northward IMF: 500h, southward IMF: 460h;
- the KHI: 35% for northward IMF, 20% for equatorial plane IMF, 10% for southward IMF.

- Several possible cross-scale energy transport mechanisms associated with the KHI:



Masson and Nykyri 2018

## ■ Cluster, MMS, THEMIS and Swarm orbits in June 2019:



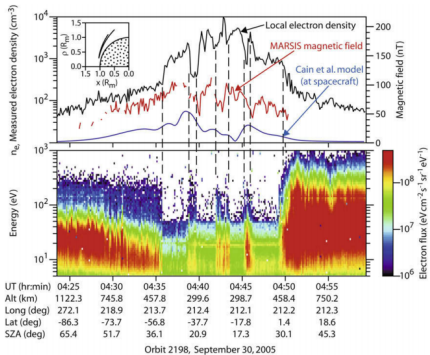
Masson and Nykyri 2018

- These new and unique observations will enable to tackle the following open questions:
- 1. What is the evolution of a Kelvin–Helmholtz vortex from birth to collapse?
- 2. How is magnetic reconnection initiated within K–H rolled-up vortices?
- 3. Do they enable solar wind plasma to enter into magnetospheres?
- 4. What is their role in the formation and existence of the cold dense plasma sheet?



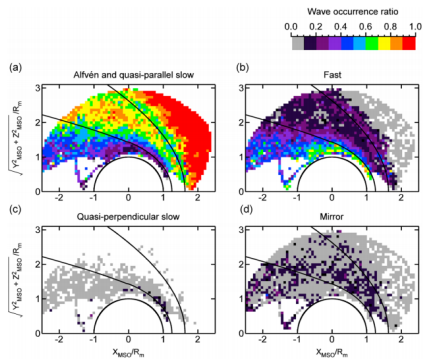
# KHI on the Martian Space Environment

- Several observations made at Mars are suggestive of the KHI operating at its ionosphere:



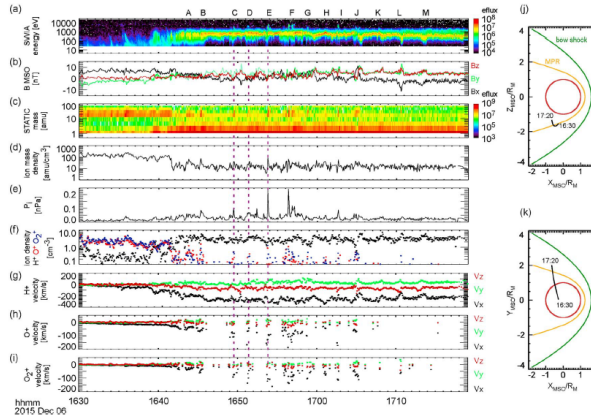
Gurnett et al. 2010(Mars Express)

WANG,XING • Group Meeting-Kelvin-Helmholtz Instability •



Ruhunusiri, Halekas, Connerney, et al.  
2015(MAVEN)

- Periodic perturbations: energy( $T \sim 3\text{min}$ , (a)A-M); magnetic field(b);
- Heavy ions( $\text{O}^+$ ,  $\text{O}_2^+$ ,(c)), $\rho \uparrow$ (d);  $p_i \uparrow$ (e);



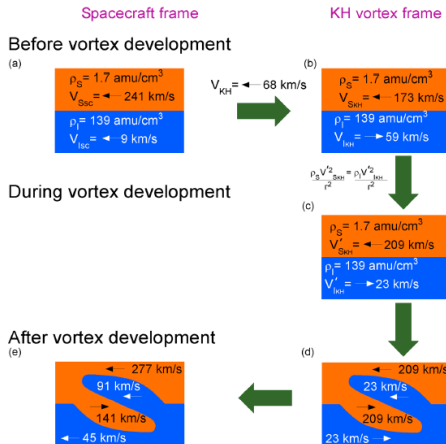
Ruhunusiri, Halekas, McFadden, et al. 2016

- At boundary:  $\rho, v_x$  of  $\text{H}^+ \downarrow$  and periodic(g),  $\rho, v_x$  of  $\text{O}^+$ ,  $\text{O}_2^+ \uparrow$ (f,h,i).



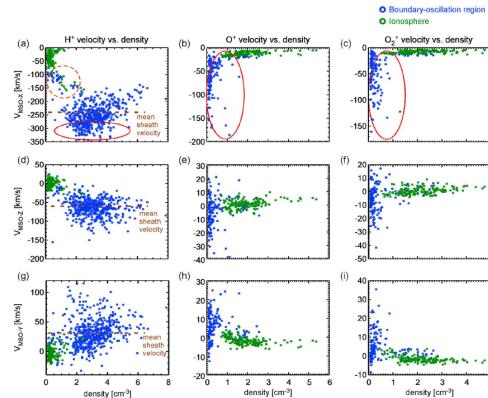
- Rolled up vortices:  $v_{magnetosphere} > v_{sheath}$ , Earth ✓, Mars ×;

### KH vortex development at Mars



Ruhunusiri, Halekas, McFadden, et al. 2016

$$\blacksquare \quad \rho_S \frac{v_{SKH}^2}{r^2} = \rho_I \frac{v_{IKH}^2}{r^2}; \quad v_{KH} = \frac{1}{2} \left( \frac{v_S + v_I}{2} + \frac{\rho_S v_S + \rho_I v_I}{\rho_S + \rho_I} \right).$$



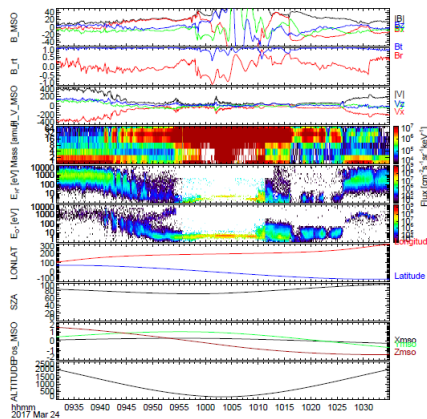
- Fully developed vortex:
  1.  $v_{xs} \uparrow < 0$ , and  $> v_{xs0}$ ;
  2.  $v_{xi} \uparrow < 0$ , and  $> v_{xi0}$ ;
  3.  $v_{xs} \downarrow > 0$ ;
  4.  $v_{xi} \downarrow < 0$ , and  $> v_{xi0}$ ;
- (a):  $v_{H^+} < 0$  and  $> v_{ms}$ , 1, 4✓;
- (b), (c):  $v_{O^+}, v_{O_2^+} < 0$  and  $> v$  in ionosphere, 2✓;
- (a):  $v_{H^+}$  in the boundary oscillation  $< 0$ , and  $< v_{ms}$ , 3×.
- Not fully rolled up!

Ruhunusiri, Halekas, McFadden, et al. 2016

- The growth rate of KHI:  $\gamma_{max} = 8 \times 10^{-3} s^{-1}$ , the spatial growth rate corresponding to the temporal growth rate:  $k_i = \frac{\gamma}{V_g} = 1.2 \times 10^{-4} km^{-1}$ ;
- Amplitude of KH vortex:  $A = A_0 e^{k_i \delta d}$ ;  $\delta d = 9100 km$ , if fully rolled up,  $A = 3A_0$ ; but  $\frac{A}{A_0} < 3$  according to Penz et al. 2004.

# Further Works

- Finding the KH waves on the Martian ionopause based on MAVEN data;
- Estimating the ion escape rate caused by KHI.



- the ion escape rate:  $f \approx \frac{n_i n_c}{T_M}$ ;
- $n_c$  is the plasma cloud number,  
 $T_M \approx 120 - 240s$ ;

Table 1  
Loss of atomic oxygen from Mars by different escape processes

Process	Loss of oxygen ( $s^{-1}$ )	Authors
Atmospheric sputtering	$4.3 \times 10^{23}$	Leblanc and Johnson (2002)
Photochemical processes	$5 \times 10^{24}$	Lammer and Bauer (1991)
Average ion pick up	$3 \times 10^{24}$	Lammer et al. (2003a)
Plasma clouds maximum	$3 \times 10^{24}$	this work
Plasma clouds minimum	$2 \times 10^{23}$	this work

Penz et al. 2004



## 参考文献 I

-  DA Gurnett et al. "Large density fluctuations in the Martian ionosphere as observed by the Mars Express radar sounder". In: *Icarus* 206.1 (2010), pp. 83–94.
-  H Hasegawa et al. "Transport of solar wind into Earth's magnetosphere through rolled-up Kelvin–Helmholtz vortices". In: *Nature* 430.7001 (2004), pp. 755–758.
-  Zachary W Henry et al. "On the dawn-dusk asymmetry of the Kelvin-Helmholtz instability between 2007 and 2013". In: *Journal of Geophysical Research: Space Physics* 122.12 (2017), pp. 11–888.
-  K-J Hwang et al. "Kelvin-Helmholtz waves under southward interplanetary magnetic field". In: *Journal of Geophysical Research: Space Physics* 116.A8 (2011).



## 參考文献 II

-  Shiva Kavosi and Joachim Raeder. "Ubiquity of Kelvin–Helmholtz waves at Earth's magnetopause". In: *Nature Communications* 6 (2015), p. 7019.
-  Dong Lin et al. "Properties of Kelvin-Helmholtz waves at the magnetopause under northward interplanetary magnetic field: Statistical study". In: *Journal of Geophysical Research: Space Physics* 119.9 (2014), pp. 7485–7494.
-  A Masson and K Nykyri. "Kelvin–Helmholtz instability: Lessons learned and ways forward". In: *Space Science Reviews* 214.4 (2018), p. 71.
-  T Penz et al. "Ion loss on Mars caused by the Kelvin–Helmholtz instability". In: *Planetary and Space Science* 52.13 (2004), pp. 1157–1167.



## 參考文献 III

-  Suranga Ruhunusiri, JS Halekas, JEP Connerney, et al. “Low-frequency waves in the Martian magnetosphere and their response to upstream solar wind driving conditions”. In: *Geophysical Research Letters* 42.21 (2015), pp. 8917–8924.
-  Suranga Ruhunusiri, JS Halekas, JP McFadden, et al. “MAVEN observations of partially developed Kelvin-Helmholtz vortices at Mars”. In: *Geophysical Research Letters* 43.10 (2016), pp. 4763–4773.
-  K Takagi et al. “Kelvin-Helmholtz instability in a magnetotail flank-like geometry: Three-dimensional MHD simulations”. In: *Journal of Geophysical Research: Space Physics* 111.A8 (2006).
-  MGGT Taylor et al. “Spatial distribution of rolled up Kelvin-Helmholtz vortices at Earth’s dayside and flank magnetopause”. In: *Annales Geophysicae*. Vol. 30. 6. 2012, pp. 1025–1035.



谢谢！